Semnan University

Mechanics of Advanced Composite Structures

journal homepage: http://MACS.journals.semnan.ac.ir

Nonlinear Bending Behavior of Functionally Graded Plates Combined with Active Fiber Composites under Thermal Environment

N. Pradhan [a], S. K. Sarangi [b*]

[a] *Department of Civil Engineering, ITER, Siksha 'O' Anusandhan (Deemed to be University), Bhubaneswar, India*
[b] *Department of Mechanical Engineering, National Institute of Technology Patna, India*

KEYWORDS

Static analysis
Functionally graded plates
Piezoelectric composites
Thermo-mechanical loading

ABSTRACT

The present paper describes the study of nonlinear bending characteristics of smart Functionally Graded (FG) plates combined with piezoelectric composites. Material properties for the base FG plate are considered to vary along the thickness direction following the power-law principle. In this analysis, commercially available active fiber composite (AFC) material is utilized as the piezoelectric composite. A finite element (FE) model is made for the FG plate combined with AFC material. Simulation models for the smart FG plates are also developed using ANSYS software taking into account the effect of temperature on the material properties. Nonlinear deformations for the smart FG plate for various values of power index and different boundary conditions are presented for thermo-mechanical loading conditions considering the properties to be temperature as well as position dependent. Efforts are made to examine the performance of AFC patches towards control of nonlinear deflections. Various configurations for the smart FG plates are considered and the best location for placing the AFC patches is identified based on the efficiency of AFC material for controlling nonlinear deformations of the FG plates.

1. Introduction

Functionally graded (FG) materials are novel materials with microscopic inhomogeneous characteristics [1,2]. One variety of these FG materials is fabricated by combining metal and ceramics to suit particular applications in which the ceramic material gives high thermal resistance while the metal constituent provides strength as well as toughness to the structure. The gradually changing volume fraction of the ingredients gives smoothly varying or graded properties to the functionally graded structures with respect to spatial coordinates [3-6] thereby tending to reduce the residual and thermal stress. This also reduces the stress concentrations which are found in the adjoining layers in conventional composite materials. Functionally graded (FG) plates are essential structural elements frequently used in leading civil as well as aerospace structures. In the recent past, piezoelectric materials are effectively been used in sensors as well as actuators in smart composite structures but the monolithic piezoelectric materials are found to have low control capability the reason being low values of their piezoelectric coefficients. It has been shown that the brittle piezoelectric fibers can be efficiently used for making polymer composites with better properties good enough for structural applications and perhaps, this has inspired researchers for developing piezoelectric composites (PZC). Effective material properties offered by these PZCs are superior to those of the piezoelectric materials [7-9]. Active Fiber Composite (AFC) material is one piezoelectric composite material that is commercially available, and this AFC provides a better and a broad range of properties as compared to the existing monolithic materials alone. Applications of these active fiber composites are seen in the defense industry and this AFC material is beneficial for its use in helicopter rotor blades which are normally noisy and may vibrate largely in flight due to high aerodynamic loading. Bent and Hagood [10] presented the use of AFC

* Corresponding author. Tel.: +7008350274
E-mail address: sarojksarangi@gmail.com

DOI: 10.22075/MACS.2021.20956.1283
Received 20-07-28; Received in revised form 20-09-18; Accepted 21-04-01

material to achieve the in-plane actuation by the piezoelectric composites.

Functionally graded materials can withstand very high thermal gradient and due to this, it is suitable for use in structures and space plane body, rocket engine component, etc. These smart FG structures may be subjected to large deflections which may lead to failure of these structures. Smart FG structures can be designed when the base structure is composed of functionally graded material for the multi-functional role such as higher fracture toughness, improved strength, reduced stress intensity factors, etc. to satisfy the high-performance requirements. Again, these FG structures play a vital role when subjected to an elevated temperature environment. Therefore, control of large deflections for these structures becomes necessary.

Panda and Ray [11] studied nonlinear static behavior of smart FG plates utilizing piezoelectric fiber-reinforced composite (PFRC) as actuator and investigated the performance of this actuator for the active deformations control of functionally graded plates. An investigation is also done to see the effects of change of fiber orientation on large deflections of FG plates. For enabling the use of FG structures under thermal environment, Praveen and Reddy [12] studied thermoelastic characteristics of the FG plates to ascertain the response of nonlinear stress and deflection of plates under thermo-mechanical loading conditions. Behjat et al. [13] developed an FE model to investigate the static and dynamic characteristics of FGPM plates under both mechanical as well as electrical loading with material property gradation in thickness direction. Following first-order shear deformation theory including thermal and piezoelectric effects, results are obtained for studying the effects of different piezoelectric materials and boundary conditions for static deformation, free vibration, and dynamic response. Panda et al. [14] studied the behavior of smart FG beams utilizing active fiber composites as actuators and investigated the performance of this actuator for the active vibration control of functionally graded beams.

Zenkour and Alghanmi [15] carried out stress and deformation analysis of FG plates integrated with faces made of piezoelectric materials and studied the influence of applied voltage, material anisotropy, and aspect ratio. Barati and Zenkour [16] studied Size-dependent forced vibration characteristics of FG nanobeams for hygro-thermal loading and uniform dynamic loads using higher-order refined beam theory. A parametric study is presented showing the importance of moisture concentration and temperature rise, material composition, and boundary conditions on the forced vibration behavior of FG nanobeams. Subsequently, Barati et al. [17] presented a dynamic analysis of nanobeams subjected to moving nanoparticles considering hygro-thermal environments. Recently, Zenkour and Radwan [18] studied the effects of moisture and temperature on the bending analysis of FG porous plates. The effects due to moisture and thermal loads on FG porous plates are discussed in this paper. So far, research work is not available regarding the control of nonlinear deformations of functionally graded plates combined with the commercially available AFC material. In this regard, the performances of AFC material on the control of large deflections of FG plate structures need to be studied.

In this research, the finite element model is developed for the smart FG plates combined with AFC materials. Simulation models for the smart FG plates are developed using ANSYS software considering the temperature-dependent material properties. The use of commercially available active fiber composite (AFC) material for large deformation control of FG plates is studied and the working of this AFC material for suppressing nonlinear deflections of smart FG plates is examined. The best location for placing the AFC patches in the smart FG plates is suggested based on the efficient working of AFC material for suppressing the nonlinear deformations of FG plates for clamped as well as simply supported boundary conditions.

2. Material Properties and Geometric Configuration

Figure 1 represents a functionally graded plate whose material properties vary continuously and smoothly in its thickness direction (z) following power-law [19] as explained below:

$$P(z) = (P_U - P_L)\left(\frac{z}{h} + \frac{1}{2}\right)^k + P_L \quad (1)$$

where 'P' denotes the properties like modulus of elasticity, density, etc. P_U and P_L denote the material properties of FG structure respectively at top-most and bottom-most surfaces, 'h' represents the thickness of the plate and 'k' represents the non-negative power-law index or material grading index which depends upon the design requirements and the change of material profile along with the thickness of the plate.

In this analysis, steel and alumina are taken as constituent materials for the FG plate in which the metal and ceramic are considered respectively for the extreme lower and upper surfaces. The constituent material properties considered here are explained in Table 1 [19].

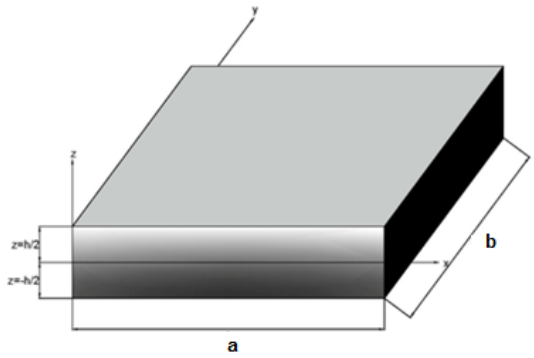

Fig. 1. Representation of Functionally Graded plate

Table 1. Properties of constituent materials for FG plate [19]

Constituent Material	Young's Modulus (E) (GPa)	Density (ρ) (Kg/m^3)	Poisson's Ratio (υ)
Steel (SUS304)	201.04	8166	0.32
Alumina (Al_2O_3)	349.55	3800	0.26

Material properties under Thermal Environment:

Functionally graded materials are very frequently used for applications involving elevated temperature conditions. Therefore, in this analysis, material properties of constituents of the FG plate are also considered for elevated temperature. For this, the material properties are considered as per the modified power-law equation as explained below:

$$P(z,T) = \left(P_u(T) - P_L(T)\right)\left(\frac{z}{h}+\frac{1}{2}\right)^k + P_L(T)$$
$$P(T) = P_0(P_{-1}T^{-1} + 1 + P_1T + P_2T^2 + P_3T^3) \quad (2)$$

in which the symbols have their usual meaning [19].

The temperature coefficients for the constituent materials are described in Tables 2 and 3. These coefficients along with the properties of constituent materials as explained in Table 1 are used for deciding the temperature and position-dependent properties of materials for the FG plate.

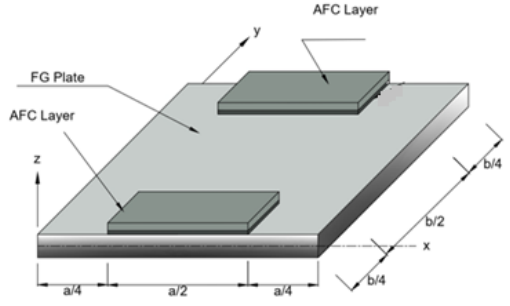

Fig. 2. Representation of smart Functionally Graded plate combined with AFC patches

Table 2. The Coefficients of Temperature for Steel [19]

Properties	P_0	P_{-1}	P_1	P_2	P_3
Thermal expansion coefficient (1/K)	12.33 ×10^{-6}	0	8.086×10^{-4}	0	0
Young's modulus (Pa)	201.04×10^9	0	3.079×10^{-4}	-6.534×10^{-7}	0
Poisson's ratio (υ)	0.326	0	-2.002×10^{-4}	3.797×10^{-7}	0
Density, ρ (Kg/m^3)	8166	0	0	0	0

Table 3. The coefficient of temperature for Alumina [19]

Material properties	P_0	P_{-1}	P_1	P_2	P_3
Thermal expansion coefficient (1/K)	6.8269 ×10^{-6}	0	1.838×10^{-4}	0	0
Young's modulus (Pa)	349.55 ×10^9	0	-3.853×10^{-4}	4.027 ×10^{-7}	-1.673×10^{-10}
Poisson's Ratio (υ)	0.26	0	0	0	0
Density, ρ (Kg/m^3)	3800	0	0	0	0

3. Finite Element Formulation

A plate composed of Functionally graded material and having dimensions '*a*' and '*b*' and is combined with Active Fiber Composite (AFC) patches of thickness 'hp' on its top surface as explained (Fig. 2).

The deformation kinematics is considered following first order shear deformation theory. The Mid-plane of the base plate is taken as a reference plane and for a point on it, u_0 and v_0 are translational displacements respectively along x and y directions. θ_x and Φ_x are rotations of normals to the mid planes of base FG plate and AFC layer, respectively about y-axis while θ_y and Φ_y are the rotations of normals about the x-axis. Loading for the present problem is considered to be distributed uniformly on the top surface of the overall FG plate. According to the deformation theory, displacements u and v of a point in the plate are expressed as

$$u(x,y,z) = u_0(x,y) + \left(z - < z - \frac{h}{2} >\right)\theta_x(x,y) + \left(< z - \frac{h}{2} - h_v >\right)\Phi_x(x,y)$$
$$v(x,y,z) = v_0(x,y) + \left(z - < z - \frac{h}{2} >\right)\theta_y(x,y) + \left(< z - \frac{h}{2} - h_v >\right)\Phi_y(x,y) \quad (3)$$

in which the singularity functions in brackets $< >$ are appropriately defined so that the displacement continuity is fulfilled between the base FG plate and the AFC layer.

Similarly, transverse displacement w can be expressed as

$$w(x,y,z) = w_0(x,y) + \left(z - < z - \frac{h}{2} > \right)\theta_z(x,y) + \left(< z - \frac{h}{2} - h_v > \right)\Phi_z(x,y) \quad (4)$$

in which w_0 denotes the transverse displacement of a point on the reference plane.

The displacement variables are arranged as translational and rotational degrees of freedom. These are explained as

$$\{d_t\} = [u_0 \;\; v_0 \;\; w_0]^T \;, \quad \{d_r\} = \left[\theta_x \;\; \theta_y \;\; \theta_z \;\; \Phi_x \;\; \Phi_y \;\; \Phi_z\right]^T \quad (5)$$

For eliminating the shear locking problem, selective integration rule is implemented.

For the plate, the strains at a point are indicated by vectors $\{\varepsilon_b\}$ and $\{\varepsilon_s\}$ as

$$\{\varepsilon_b\} = \left[\varepsilon_x \;\; \varepsilon_y \;\; \varepsilon_{xy} \;\; \varepsilon_z\right]^T, \quad \{\varepsilon_s\} = \left[\varepsilon_{xz} \;\; \varepsilon_{yz}\right]^T \quad (6)$$

where ε_x, ε_y and ε_z denote normal strains; ε_{xy} denote in-plane shear strain; ε_{xz} and ε_{yz} denote the transverse shear strains.

Utilizing Von Kármán equations in association with Eq. (6) along with displacement field explained by Eqs. 3 and 4, strain corresponding to a point in the plate system are written as

$$\{\varepsilon_b\}_k = \{\varepsilon_{bt}\} + [Z_1]\{\varepsilon_{br}\} + \{\varepsilon_{bnr}\}, \quad \{\varepsilon_s\}_k = \{\varepsilon_{st}\} + \{Z_2\}\{\varepsilon_{sr}\}, \quad k = 1$$
$$\{\varepsilon_b\}_k = \{\varepsilon_{bt}\} + [Z_3]\{\varepsilon_{br}\} + \{\varepsilon_{bnr}\}, \quad \{\varepsilon_s\}_k = \{\varepsilon_{st}\} + \{Z_4\}\{\varepsilon_{sr}\}, \quad k = 2 \quad (7)$$

in which the strain vectors $\{\epsilon_b\}$ and $\{\epsilon_s\}$ are representing the state of strain.

The subscript k as 1 or 2 in Eq. 7 defines the strains for base FG plate or AFC patch respectively.

Maintaining consistency with the representation of strains, the stresses in the plate system are written as

$$\{\sigma_b\} = \left[\sigma_x \;\; \sigma_y \;\; \sigma_{xy} \;\; \sigma_z\right]^T, \quad \{\sigma_s\} = [\sigma_{xz} \;\; \sigma_{yz}]^T \quad (8)$$

where σ_x, σ_y, σ_z denote normal stresses; σ_{xy} denotes in-plane shear stress; σ_{xz}, σ_{yz} are transverse shear stresses.

The constitutive equations for the base FG plate are written as

$$\{\sigma_b{}^k\} = \left[\bar{C}_b{}^k\right](\{\varepsilon_b{}^k\} - \{\propto\}\Delta T), \quad \{\sigma_s{}^k\} = \left[\bar{C}_s{}^k\right]\{\varepsilon_s{}^k\}, k = 1 \quad (9)$$

and those for the AFC are

$$\{\sigma_b{}^k\} = \left[\bar{C}_b{}^k\right]\{\varepsilon_b{}^k\} - \{\bar{e}_b\}E_x, \quad \{\sigma_s{}^k\} = \left[\bar{C}_s{}^k\right]\{\varepsilon_s{}^k\}, \quad D_x = \{\bar{e}_b\}^T\{\varepsilon_b{}^k\} + \bar{\varepsilon}_{33}E_x \;, k = 2 \quad (10)$$

where $\bar{\epsilon}_{33}$ is the transformed dielectric constant of the AFC material and the elastic coefficient matrices for FG plate (*k=1*) and AFC material (*k=2*) are written as

$$\left[\bar{C}_b^k\right] = \begin{bmatrix} \bar{C}_{11}^k & \bar{C}_{12}^k & \bar{C}_{16}^k & \bar{C}_{13}^k \\ \bar{C}_{12}^k & \bar{C}_{22}^k & \bar{C}_{26}^k & \bar{C}_{23}^k \\ \bar{C}_{16}^k & \bar{C}_{26}^k & \bar{C}_{66}^k & \bar{C}_{36}^k \\ \bar{C}_{13}^k & \bar{C}_{23}^k & \bar{C}_{36}^k & \bar{C}_{33}^k \end{bmatrix}, [\bar{C}_s^k] = \begin{bmatrix} \bar{C}_{55}^k & \bar{C}_{45}^k \\ \bar{C}_{45}^k & \bar{C}_{44}^k \end{bmatrix},$$

$$\{\bar{e}_b\} = [\bar{e}_{31} \quad \bar{e}_{32}\bar{e}_{36} \quad \bar{e}_{33}]^T$$

and the matrices ($\{\bar{e}_b\}$ and $\{\bar{e}_s\}$) are expressed as $\{\bar{e}_b\} = [\bar{e}_{31} \quad \bar{e}_{32}\bar{e}_{36} \quad \bar{e}_{33}]^T$ and

$$\{\bar{e}_s\} = [\bar{e}_{35} \quad \bar{e}_{34}]^T$$

In the above expressions, the elastic coefficient matrices for the FG plate are expressed as functions of z.

The electric field is expressed as $E_x = -V/h_p$ where V is the voltage supplied to the AFC patches. Discretization of the model is performed by eight node isoparametric elements and nodal displacements for any node (I = 1, 2, 3, .,, , 8) are written as

$$\{d_{ti}\} = [u_{0i} \quad v_{0i} \quad w_{0i}]^T, \quad \{d_{ri}\} = [\theta_{xi} \quad \theta_{yi} \quad \theta_{zi}\Phi_{xi} \quad \Phi_{yi} \quad \Phi_{zi}]^T \quad (11)$$

The displacement variables at a point are given by

$\{d_t\} = [N_t]\{d_t^e\}$ and

$\{d_r\} = [N_r]\{d_r^e\}$ in which, the vectors $\{d_t^e\}$, $\{d_r^e\}$, $[N_t]$ and $[N_r]$ are defined as follows:

$$\{d_t^e\} = [\{d_{t1}^e\}^T \quad \{d_{t2}^e\}^T \; . \; . \; . \quad \{d_{t8}^e\}^T]^T, \quad \{d_r^e\} = [\{d_{r1}^e\}^T \quad \{d_{r2}^e\}^T \; . \; . \; . \quad \{d_{r8}^e\}^T]^T,$$
$$[N_t] = [N_{t1} \quad N_{t2} \; . \; . \; . \quad N_{t8}]^T, \quad [N_r] = [N_{r1} \quad N_{r2} \; . \; . \; . \quad N_{r8}]^T, \quad N_{ti} = n_i I_t \; and \; N_{ri} = n_i I_r \quad (12)$$

In Eq. 12, It and Ir represent 3 × 3 and 9 × 9 identity matrices; n_i (i = 1,2,3, … ,8) are shape functions for natural coordinates for i^{th} node. Strain vectors $\{\varepsilon_{bt}\}$, $\{\varepsilon_{br}\}$, $\{\varepsilon_{bnr}\}$, $\{\varepsilon_{st}\}$ and $\{\varepsilon_{sr}\}$ at a point in the element can be written as

$$\{\varepsilon_{bt}\} = [B_{tb}]\{d_t^e\}, \{\varepsilon_{br}\} = [B_{rb}]\{d_r^e\}, \quad \{\varepsilon_{bnr}\} = \frac{1}{2}[B_1][B_2]\{d_t^e\} \quad (13)$$
$$\{\varepsilon_{st}\} = [B_{ts}]\{d_t^e\}, \{\varepsilon_{sr}\} = [B_{rs}]\{d_r^e\}$$

where $[B_{tb}]$, $[B_{rb}]$, $[B_{ts}]$, $[B_{rs}]$, $[B_1]$ and $[B_2]$ are the nodal strain displacement matrices.

Principle of minimum potential energy given as $\delta T_p{}^e = 0$ is used and the equilibrium equations for an element are written as follows:

$$[K_{tt}^e]\{d_t^e\} + [K_{tr}^e]\{d_r^e\} = \{F_t^e\} + \left(\{F_{tp}^e\} + \{F_{tpn}^e\}\right)V \quad (14)$$

$$[K_{rt}^e]\{d_t^e\} + [K_{rr}^e]\{d_r^e\} = \{F_r^e\} + \{F_{rp}^e\}V \quad (15)$$

Note that for the element not combined with AFC material, the matrices $\{F^e_{tp}\}$, $\{F^e_{tpn}\}$ and $\{F^e_{rp}\}$of Eqs. (14) and (15) are null matrices.

The elemental equilibrium equations are then assembled to get the global equations as

$$[K_{tt}]\{X_t\} + [K_{tr}]\{X_r\} = \{F_t\} + (\{F_{tp}\} + \{F_{tpn}\})V \quad (14)$$

$$[K_{rt}]\{X_t\} + [K_{rr}]\{X_r\} = \{F_r\} + \{F_{rp}\}V \quad (15)$$

Here $[K_{tt}]$, $[K_{tr}]$, $[K_{rt}]$ and $[K_{rr}]$are global matrices for stiffness, $\{F_{tp}\}$, $\{F_{tpn}\}$and $\{F_{rp}\}$ are global coupling vectors, $\{X_t\}$ and $\{X_r\}$ are the nodal displacement vectors and$\{F_t\}$and $\{F_r\}$ are the global nodal mechanical force vectors.

4. Development of Simulation Model

For the smart functionally graded plate, a simulation model is developed in ANSYS (APDL) environment. Shell 281 (8 node) element is chosen for the discretization of the model as this element is most suited to analyze thin to moderately thick structures with lay-up options and possesses the ability for modeling composite as well as functionally graded structures with layered applications to carry out linear and nonlinear analysis. This element is also having the capability to accurately model layers with different material properties. Functionally graded plate considered here for analysis is made up of steel (metal) and alumina (ceramic), where the bottom surface of the substrate FG plate is considered to be metal-rich and the top surface to be ceramic rich. The properties of the constituent materials of the FG plate are mentioned in Table 1. Accordingly, the varying Young's modulus (E) and density (ρ) in the direction of the FG plate thickness for negligible temperature variation are computed and are presented in Fig. 3 for different power-law indexes. Note that desired variation of properties for the FG plate is obtained using a specific value of power-law index.

A simulation model is developed in ANSYS for the smart FG plate considering various layers for the substrate FG plate. For this, a convergence analysis has been carried out to optimize the number of layers essential to represent the substrate FG plate. Table 4 describes this convergence study for clamped as well as simply supported boundary conditions for the simulation model. It can clearly be seen from this table that ten layers can be considered for developing the model and hence onwards ten layers are considered for developing the models for the FG substrate plate. The material properties for the various layers for the FG structure considered are calculated following the procedure as outlined earlier in section 2 incorporating both the temperature and position variation along with the thickness. Next discretization of the model is carried out and Fig. 4 illustrates the discretized model for the FG plate using shell 281 elements. Also, an optimum mesh size is decided based on the convergence study and for the sake of brevity which details are not presented here.

Table 4. Convergence analysis for optimizing the number of layers

No. of Layers	Maximum nonlinear non-dimensional deflection ($\acute{w} = \frac{w}{h}$)	
	Clamped-Clamped	Simply Supported
5	0.516	0.215
10	0.562	0.223
15	0.562	0.223
20	0.562	0.223

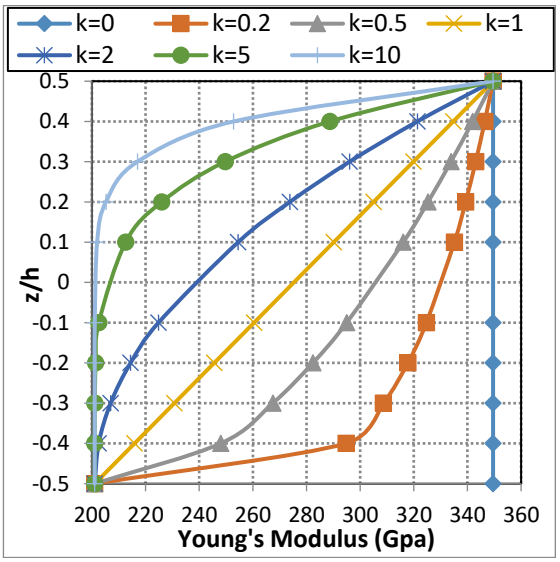

(a)

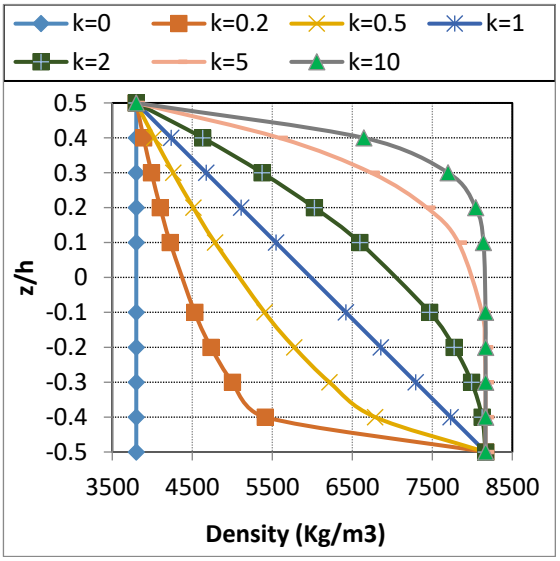

(b)

Fig. 3. Variation of (a) Young's modulus (b) density along with plate thickness for different power-law index (k).

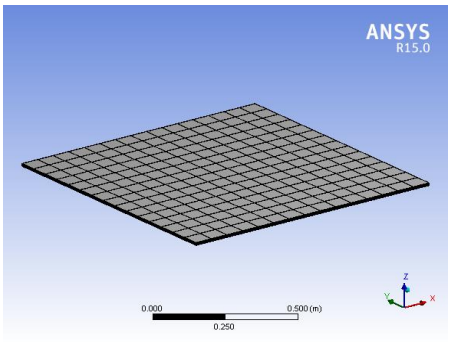

Fig. 4. ANSYS Simulation model for FG plate.

5. Results and Discussion

In this section, results are computed taking the models developed in the previous sections. The Material properties calculated as described in section 2 are used to find the results. Active fiber composite is used as the piezoelectric composite material and its effective properties considered here are [20]

C11 = 138.1 GPa, C12 = 75.15 GPa, C22 = 148.9 GPa, C66 = 39.14 GPa, e31 = -5.2 C/m^2, e33 = 15.1 C/m^2, e15 = 12.7 C/m^2. The density of AFC material is taken as 6400 kg/m3.

First, the models developed in the previous sections are validated and for this appropriate boundary conditions are employed in ANSYS. Nonlinear center deflections are calculated for the functionally graded plate under uniform loading conditions and the deflections computed by the ANSYS simulation model are correlated with the published results [21] for various values of power index. For this comparison, the material properties and dimensions for the FG plate for the ANSYS simulation model are taken according to those mentioned in the literature [21]. Table 5 explains the comparison and verifies the present ANSYS simulation model. Using the ANSYS model developed the maximum values of dimensionless transverse deformation for the FG plate for various power index values and boundary conditions are computed and presented in Table 6. It may be noticed that deflection value increases with higher power-law index values for both clamped (CC) and simply supported (SS) boundary conditions.

Table 5. Center deflection $\left(\dot{w} = \frac{w}{h}\right)$ for the FG plate for different mess size and various power-law index (k)

k	Mesh size (a/h = 5)	Ref. [21]	Present (ANSYS)
0.5	2 x 2	0.0357	0.0364
	4 x 4	0.0336	0.0339
1	2 x 2	0.0394	0.0402
	4 x 4	0.0373	0.0392
2	2 x 2	0.0430	0.0441
	4 x 4	0.0409	0.0415

Table 6. Maximum transverse deflection (w/h) of FG substrate plate without AFC patches for various power exponent (k)

k	0		0.2		0.5		1		2		5		10	
B.C.	CC	SS	CC	SS	CC	SS	CC	SS	CC	SS	CC	SS	CC	SS
w/h	0.598	0.217	0.621	0.239	0.646	0.246	0.673	0.254	0.696	0.263	0.718	0.274	0.733	0.284

The linear and nonlinear transverse deformations (w/h) for the FG plate are calculated considering clamped (CC) and simply supported (SS) boundary conditions and explained in Fig. 5. It may be noticed from Fig. 5(a) that in the case of the clamped plate, the nonlinearity is significant when the deflection value (w/h) becomes greater than 0.3, and to deal with sufficient nonlinearity, deflection (w/h) can be considered as 0.6 or higher. Similarly, for the simply supported FG plate (Fig. 5(b)), the value of deflection (w/h) indicating an involvement of sufficient nonlinearity decides that a vertical pressure load 18000 N/m^2 may be used for the top surface of the plate for computing nonlinear deflections.

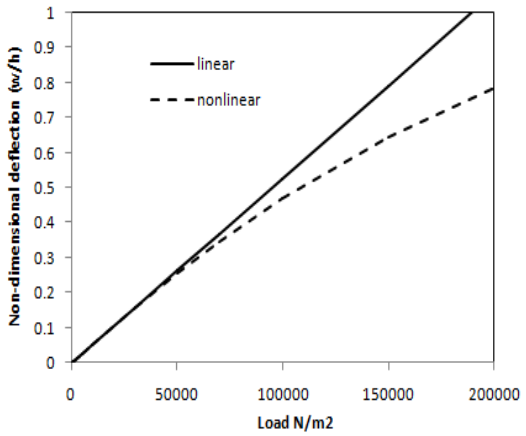

(a)

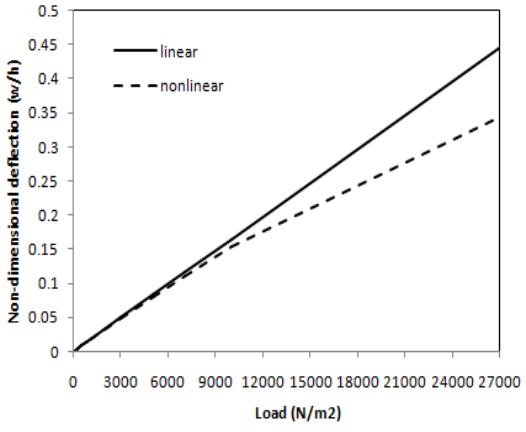

(b)

Fig. 5. Load-deformation diagram of FG plate (a) Clamped (b) Simply supported

The model developed for the smart FG plate is established by matching the computed results with the results available in the literature [11]. The nonlinear study is accomplished and the dimensions and material properties of the smart FG plate for the comparison are considered according to those in the literature [11] for the FE model and ANSYS simulation model. Fig. 6 explains the nonlinear deflection characteristics for the smart FG plates for the inactivated (V=0) and activated (V≠0) AFC patches and subjected to mechanical loading. The comparison explained in Fig. 6 indicates the agreed results and thereby validates the present methods of modeling the smart functionally graded (FG) plates.

The analysis is performed taking the smart FG plate combined with AFC patches. The properties of FG ingredients and AFC material considered here are as mentioned earlier. To examine the performance of AFC patches used as actuators for suppressing nonlinear deflections of the FG plates, results are obtained. For this purpose, FG plates combined with patches of active fiber composite material are considered in four different configurations taking the total size of AFC patches the same in all cases. Fig. 7 illustrates a square smart FG plate whose top surface is combined with four square AFC patches of equal size in different configurations. When voltage is applied externally through the piezoelectric patches, the overall FG plate behaves as a smart functionally graded plate. The total length and width of AFC patches here (Fig. 7) are taken 50% of the plate size while the thickness of the AFC patch is hp. For the computation of results, the thickness of substrate FG plate and AFC material are considered as 10 mm and 1.5 mm respectively, and the substrate plate is taken to be of a square size of side 1m.

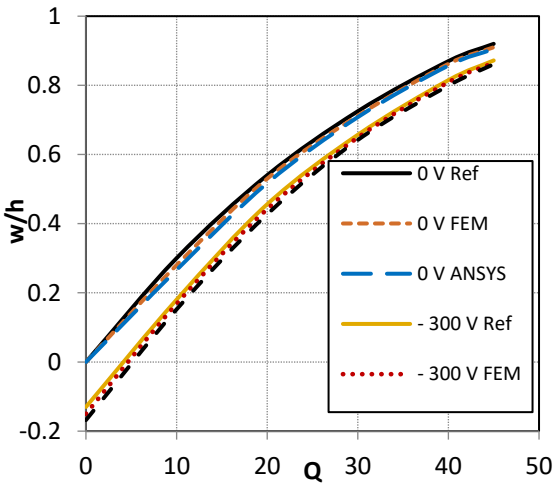

Fig. 6 Central deflection for the smart FG plate subjected to mechanical load for the FE model and the ANSYS simulation model (a=b, k=5).

Transverse deflections are obtained corresponding to different power-law index values using passive (V=0) and active (V≠0) AFC patches. The non-dimensional parameters used here for displaying the results are

$$Q = \frac{Ps^4}{E_U} \quad \text{and} \quad \hat{w} = \frac{w}{h}$$

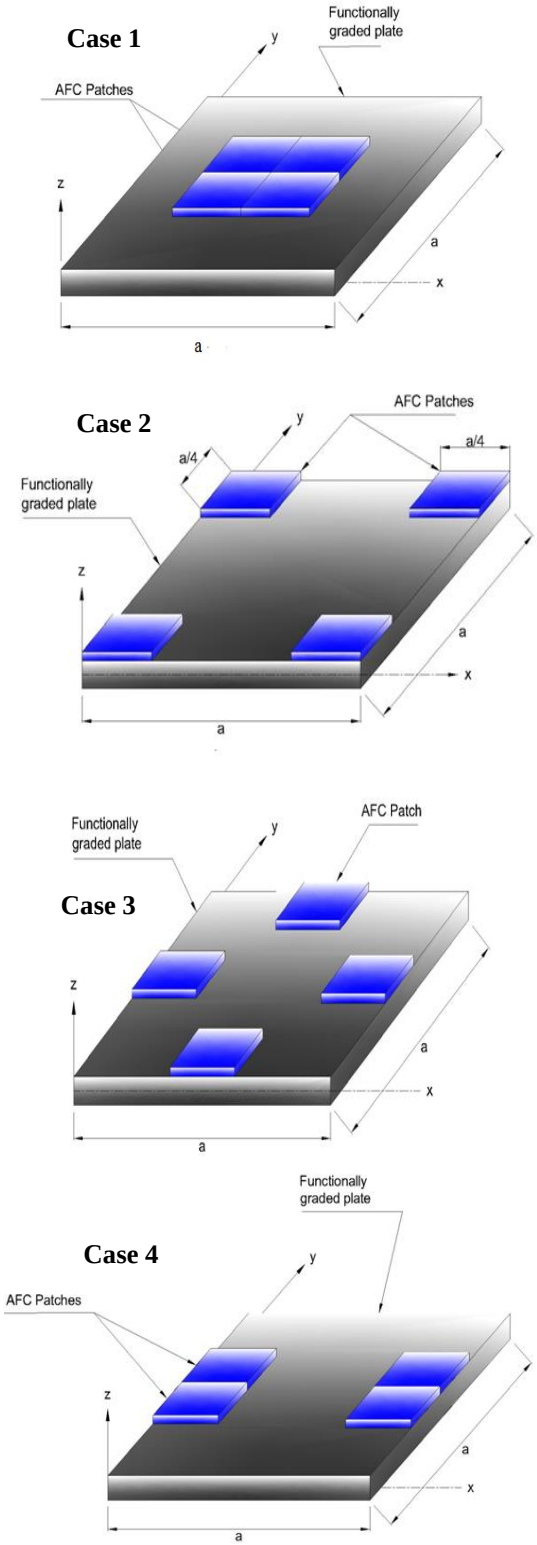

Fig. 7 Representation of smart FG plates combined with AFC patches in different configurations.

where P is the mechanical load applied uniformly on the plate's top surface and 's' is the aspect ratio. EU is the modulus of elasticity for the uppermost surface of the substrate FG plate. The simply supported and clamped boundary conditions adopted to obtain the results are as explained below:

Simply Supported (SS)

For $x = 0,\ a \rightarrow v_0 = w_0 = \theta_y = \theta_z = \emptyset_y = \emptyset_z = 0$

For $y = 0,\ b \rightarrow u_0 = w_0 = \theta_x = \theta_z = \emptyset_x = \emptyset_z = 0$

Clamped–Clamped (CC)

At $x = 0,\ a \rightarrow u_0 = v_0 = w_0 = \theta_x = \theta_y = \theta_z = \emptyset_x = \emptyset_y = \emptyset_z = 0$

At $y = 0,\ b \rightarrow u_0 = v_0 = w_0 = \theta_x = \theta_y = \theta_z = \emptyset_x = \emptyset_y = \emptyset_z = 0$

The performance of AFC patches towards the reduction of nonlinear deformation of FG plates is studied for all four different cases. For this load-deflection curves are obtained in the nonlinear range for the smart FG plate having AFC patches in four different configurations as described in Fig. 7. Fig. 8 shows the central deflection of Clamped (CC) smart FG plate when AFC patches are placed in four different configurations under the application of mechanical load for passive and active patch conditions. It can be noticed from the plots of Fig. 8 that when the patches are placed according to that of case 3 of Fig. 7, the performance of active AFC patches seems to be maximum towards control of nonlinear deformations of the FG plates.

Considering the best position for placing the AFC patches on the top surface of the FG plate, the performance of these patches for controlling nonlinear deflections of the FG plates are investigated for various control voltages and these are explained in Figs. 9 and 10 respectively for the clamped as well as simply supported FG plates.

The functionally graded plate studied here for analysis is also modeled for thermal environment following the procedure explained in section 2. The smart FG plate is modeled for a uniform temperature T = 500 K in which $T = T_0 + \Delta T$, T_0 being the installation temperature and ΔT is the uniform increase of temperature. Material properties used in the development of this model for the thermal environment are also discussed in section 2. The top surface of the plate is loaded with a pressure load. First, the maximum transverse deflections for the FG plate are obtained for various values of power-law index when the plate is subjected to both temperature and mechanical loading. These results are given in Table 7 and for the increase of power-law index values, increased deflection is observed. By comparing the results presented in Tables 6 and 7, it can be noticed that the deformation of FG plate is considerably higher for applied thermo-mechanical loading than that obtained when the plate is subjected to mechanical load only which indicates softening behavior of the plates in elevated temperature condition.

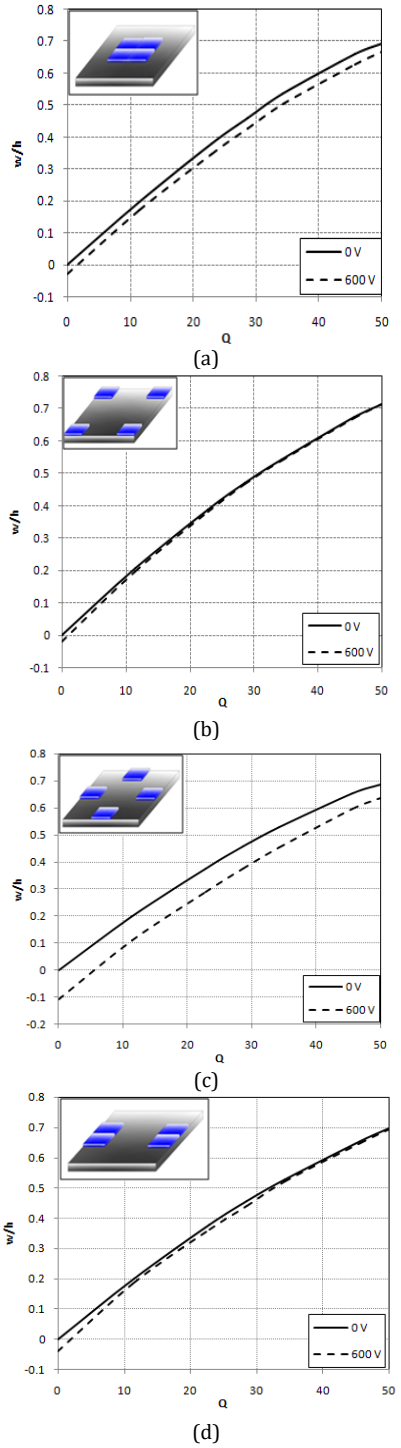

Fig. 8. Center deflections of smart FG plate with mechanical load (Q) applied when AFC patches are placed in different configurations (Clamped).

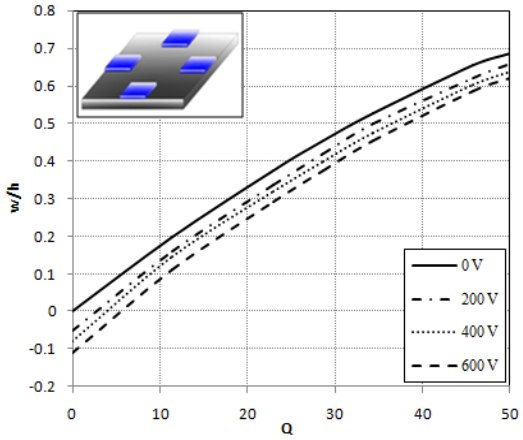

Fig. 9. Center deflections of clamped smart FG plate with applied mechanical load (Q) for various control voltages.

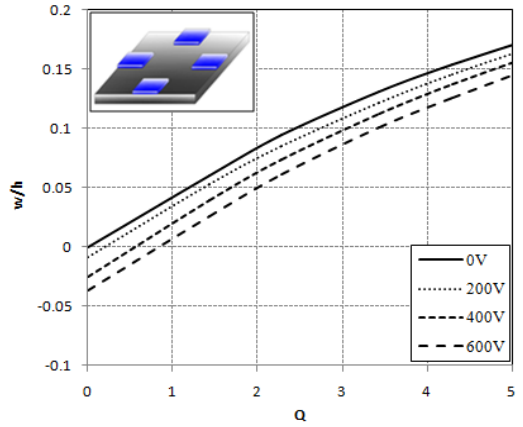

Fig. 10. Center deflections of simply supported smart FG plate with applied mechanical load (Q) for various control voltages.

Table 7. Maximum transverse deflection (w/h) for the FG substrate plate for applied Thermo-mechanical loading.

k	0		0.2		0.5		1		2		5		10	
B.C.	CC	SS	CC	SS	CC	SS	CC	SS	CC	SS	CC	SS	CC	SS
w/h	0.605	0.241	0.663	0.260	0.685	0.266	0.706	0.273	0.725	0.279	0.744	0.29	0.756	0.298

The performances of AFC patches when placed in the best location (case 3 of Fig. 7) of the FG plate under clamped and simply supported boundary conditions for various power indexes in elevated temperature condition are investigated and presented in Figs. 11 and 12 respectively. The voltage used for the AFC patches is indicated in these Figures and it can be observed that the AFC patches largely contribute towards deflection control of the FG plates.

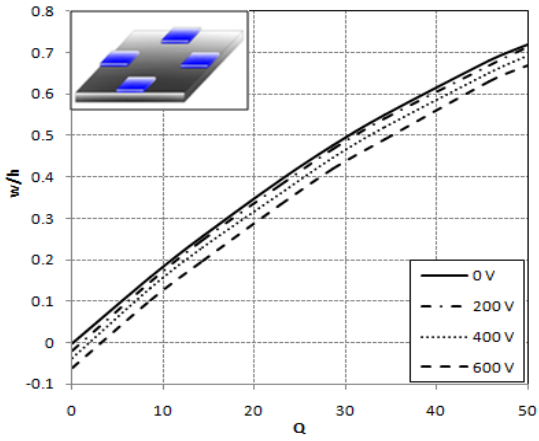

Fig. 11. Center deflection of smart FG plate subjected to thermo-mechanical loading (CC).

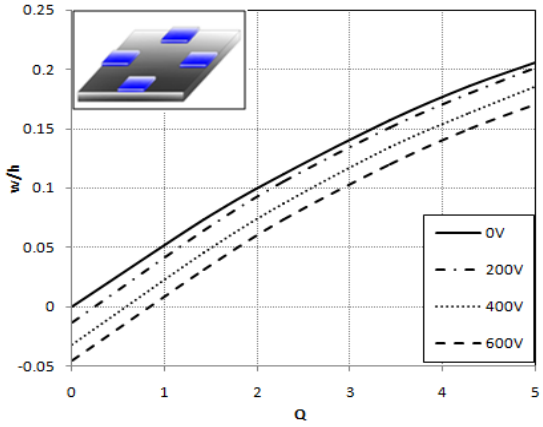

Fig. 12. Central deflection of smart FG plate subjected to thermo-mechanical loading (SS).

6. Conclusions

Smart functionally graded (FG) plate analysis is carried out and an FE model is developed for the investigation of performances of active fiber composite for suppressing the nonlinear deformations of these FG plates combined with AFC material. Von Kármán nonlinear strain displacement equations are used along with FSDT for developing a model for the structure and simulation models are developed using ANSYS software for the smart FG plates. Different boundary conditions and power-law indexes are used for evaluations of numerical results. The smart FG plate is also analyzed for high-temperature applications considering the temperature-dependent material properties using temperature coefficients. The computed results indicate that the nonlinear deflections of the smart FG plates are higher for the case of thermo-mechanical loading when compared to only mechanical loading for both clamped as well as simply supported boundary conditions indicating softening behavior of the plates in elevated temperature condition. It is observed that the active AFC patches perform satisfactorily to control the nonlinear

deformations of these smart FG plates. The optimum placement of AFC patches is also obtained for getting the best control of deformation of the FG plates in nonlinear range for both clamped and simply supported boundary conditions.

References

[1] Yamanouchi, M., Koizumi, M., Hirari, T. and Shiota, I., 1990, "Functionally graded materials", *Proceedings First International Symposium*, pp. 5-10.

[2] Koizumi, M., 1993, "The concept of FGM", *Ceramic Transactions., Functionally graded materials*, Vol. 34, pp. 3-10.

[3] Sata, N., 1993, "Characteristic of SiC-TiB2 composites as the surface layer of SiC-TiB2-Cu Functionally gradient material produced by self-propagating high-temperature synthesis", *Ceramic Transactions, Functionally graded materials*, vol. 34, pp. 109-116.

[4] Yamaoka, H., Yuki, K., Tahara, K., Irisawa, T., Watanabe, R. and Kawasaki, A., 1993, "Fabrication of functionally gradient material by slurry stacking and sintering process", *Ceramic Transactions, Functionally gradient materials*, vol. 34, pp. 165-172.

[5] Rabin, B. H. and Heaps, R. J., 1993, "Powder processing of Ni-Al2O3 FGM", Ceramic *Transactions, Functionally gradient materials,* vol. 34, pp. 173-180.

[6] Fukui, Y., 1991, "Fundamental investigation of functionally gradient material manufacturing system using centrifugal force", *International Journal of Japan society mechanical engineers Series-III*, vol. 34, pp. 144-148.

[7] Bajpai, R. B., 2011, "Applications of smart materials in present day engineering", *The Journal of Department of Applied Sciences & Humanities,* Vol. XI, pp. 8-10.

[8] Ray, M. C. and Mallik, N., 2005, "Performance of smart damping treatment using piezoelectric fiber reinforced composites", *AIAA journals*, Vol. 45, pp. 184-193.

[9] Gentilman, R., McNeal, K., Schmidt, G., Piezzochero, A. and Rossetti George, A., 2003, "Enhanced performance active fiber composites", *Smart Materials and Structures*, Vol. 5054, pp. 350-359.

[10] Bent, A. A. and Hagood, N. W., 1997, "Piezoelectric fiber composites with integrated electrodes", *Journal of* Intelligent *Material Systems and Structures*, Vol. 8, pp. 903-919.

[11] Panda, S., and Ray, M.C., 2006, "Nonlinear analysis of smart functionally graded plates integrated with a layer of piezoelectric fiber reinforced composite, *Smart materials and structures*, vol. 15(6), pp. 1595-1604.

[12] Praveen, G.N., and Reddy, J.N., 1998, "Nonlinear transient thermoelastic analysis of functionally graded ceramic-metal plates", *Int. J. solids structures*, vol. 35 (33), pp. 4457-4476.

[13] Behjat, B., Salehi, M., Armin, A., Sadighi, M. and Abbasi, M., 2011, "Static and dynamic analysis of functionally graded piezoelectric plates under mechanical and electrical loading", *ScieitnaIranica*, vol. 18(4), pp. 986-994.

[14] Panda, R. K., Nayak, B., and Sarangi, S. K., 2016 "Active vibration control of smart functionally graded beams", *Procedia Engineering*, vol. 144, pp. 551-559.

[15] Zenkour, A. M. and Alghanmi, R. A., 2019, "Stress analysis of a functionally graded plate integrated with piezoelectric faces via a four-unknown shear deformation theory", *Results in Physics*, Vol. 12, pp. 268-277.

[16] Barati, M.R. and Zenkour, A., 2018, "Forced vibration of sinusoidal FG nanobeams resting on hybrid Kerr foundation in hygrothermal environments", *Mechanics of Advanced Materials and Structures*, Vol. 25(8), pp. 669-680.

[17] Barati, M.R., Faleh, N. M. and Zenkour, A.M., 2019, "Dynamic response of nanobeams subjected to moving nanoparticles and hygro-thermal environments based on nonlocal strain gradient theory", *Mechanics of Advanced Materials and Structures*, Vol. 26(19), pp. 1661-1669.

[18] Zenkour, A.M. and Radwan, A.F., 2019, "Bending response of FG plates resting on elastic foundations in hygrothermal environment with porosities", *Composite Structures*, Vol. 213, pp. 133-143.

[19] Trinh, L.C., Vo, T.P., Thai, H., and Nguyen, T.K., 2016, "An analytical method for the vibration and buckling of functionally graded beams under mechanical and thermal loads" *Composites part-B*, vol. 100, pp. 152-163.

[20] Sarangi, S. K. and Basa, B., 2014, "Nonlinear Finite Element Analysis of Smart Laminated Composite Sandwich Plates", *International Journal of Structural Stability and Dynamics*, Vol. 14, 1350075.

[21] Talha, M. and Singh, B.N., 2010, "Static response and free vibration analysis of FGM plates using higher-order shear deformation theory", *Applied mathematical modeling*, Vol. 34, pp.3991-4011.